

Turbulence Transition and the Edge of Chaos in Pipe Flow

Tobias M. Schneider,¹ Bruno Eckhardt,¹ and James A. Yorke²

¹*Fachbereich Physik, Philipps-Universität Marburg, Renthof 6, D-35032 Marburg, Germany*

²*University of Maryland, College Park, Maryland, USA*

The linear stability of pipe flow implies that only perturbations of sufficient strength will trigger the transition to turbulence. In order to determine this threshold in perturbation amplitude we study the *edge of chaos* which separates perturbations that decay towards the laminar profile and perturbations that trigger turbulence. Using the lifetime as an indicator and methods developed in (Skufca et al, Phys. Rev. Lett. **96**, 174101 (2006)) we show that superimposed on an overall $1/\text{Re}$ -scaling predicted and studied previously there are small, non-monotonic variations reflecting folds in the edge of chaos. By tracing the motion in the edge we find that it is formed by the stable manifold of a unique flow field that is dominated by a pair of downstream vortices, asymmetrically placed towards the wall. The flow field that generates the edge of chaos shows intrinsic chaotic dynamics.

PACS numbers: 47.20.Ft, 47.20.-k

Keywords:

The transition to turbulence in pipe flow has puzzled scientists for more than 100 years because, in contrast to many other flow situations, the laminar profile is stable for all Reynolds numbers and there is no linear instability that could trigger the transition [1, 2, 3, 4]. Many experiments have therefore focussed on the determination of the ‘double threshold’ [5, 6, 7] in Reynolds number and perturbation amplitude that has to be crossed in order to trigger turbulence. Experimental studies quote a variety of values for the Reynolds numbers that have to be exceeded before sustained turbulence can be observed [3, 6]. They also support a $1/\text{Re}$ scaling for the threshold amplitude [8]. On the theoretical side, numerical studies have shown that for sufficiently high Reynolds numbers a variety of 3-d persistent flow structures of travelling wave type appear in saddle-node bifurcations. For instance, six symmetrically arranged downstream vortices appear near $\text{Re} = 1250$ [9, 10, 11]. The critical amplitude has been estimated from an analysis of the nonnormal amplification combined with an asymptotic analysis of the equations of motion; it gives a scaling of the critical amplitude like $1/\text{Re}$ for large Reynolds numbers [7, 12]. For simple models of shear flows, more detailed studies have been possible [13, 14, 15]. In particular, it has been possible to track the dynamics at the edge of chaos which separates initial conditions that decay directly to the laminar profile and those that swing up to turbulent dynamics [16]. We here apply these ideas to pipe flow, thus contributing to the elucidation of the key structures in the state space of pipe flow that are responsible for the transition between laminar and turbulent dynamics. The study is part of the dynamical system scenario advocated for the transition [4, 17], and can be related to similar observations in other shear flows, such as plane Poiseuille flow [18, 19] and plane Couette flow.

In order to identify the border between laminar and turbulent behavior we use the lifetime of perturbations as an indicator [20, 21]. The lifetime of a perturbation is defined as the time it takes to come sufficiently close to

the laminar profile where ‘sufficiently close’ is defined by the requirement that the future evolution is governed by the linearized equations of motion, which guarantees that it will asymptotically decay. Within the dynamical system picture of the transition this defines a target region around the point in state space that corresponds to the laminar profile. For the initial conditions we mimic the experimental protocol, where the type of perturbation (jets, blowing and suction, periodic modulation, etc.) is predetermined by the setup and where the strength of the perturbation is usually controlled with one parameter. We therefore pick a spatial structure for the velocity field and modify its amplitude, thereby scanning the state space along a ray. The perturbation we consider here is a pair of vortices as in the optimally growing modes identified by Zikanov [22], modulated in streamwise direction by applying a z -dependent tilt in order to break translational symmetry:

$$\mathbf{u}_0(r, \varphi, z) = \mathbf{u}_{\text{Zik}} \left(r, \varphi + \varphi_0 \sin \left(\frac{2\pi}{L} z \right), z \right), \quad (1)$$

where \mathbf{u}_{Zik} is Zikanov’s mode and L is the length of the computation domain used in our direct numerical simulation. In addition to initial conditions generated from Zikanov modes we also used initial conditions taken from a turbulent run at higher Re , as in the entry for the March 2006 Gallery of Nonlinear Images [23], and obtained convergence to the same dynamics.

For the numerical simulations we used a pseudospectral code with about $1.2 \cdot 10^5$ degrees of freedom as in [24]. The code was verified by reproducing linear theory, turbulent statistics at higher Reynolds numbers and the nonlinear evolution of Zikanov modes [22]. The length of the computational domain is $L = 10R$ and times are given in units of R/U_{cl} , where R is the radius of the pipe and U_{cl} the center velocity of the parabolic profile with the same mean flux. For the current study we note that a turbulent run up to an observation time of $1000 R/U_{cl}$ takes almost 24 hours on an 1.5 GHz IBM Power5 proces-

sor. More than 4000 integration runs have been carried out.

A typical variation of the lifetimes with amplitude of the perturbation at fixed Re is shown in Fig. 1. In regions with short lifetimes the flow relaxes quickly to the laminar profile. Towards the boundaries of these regions the lifetimes increase quickly and reach plateaus at the maximal integration time. Magnifications of the plateau regions show chaotic and unpredictable variations of lifetimes [21]. The cliff-structure in the lifetimes suggested the name *edge of chaos* for the points at the boundary between regions of smooth and of unbounded chaotic lifetime variations, respectively [16].

The steep increase in lifetimes allows for an accurate tracking of the edge of chaos under variations of Reynolds number, see Fig. 2. The edge of chaos lies in an interval in amplitude bounded by one initial condition which decays towards the laminar profile within the observation time of 1000 units and one that swings up to the turbulent flow. That the upper trajectory becomes turbulent is also verified by monitoring its energy content. The widths of the intervals is smaller than the size of the symbols. For Fig. 2 the amplitude has been multiplied by Re in order to take out the asymptotic $1/Re$ scaling [8, 12]. In view of the low Reynolds numbers and limited range accessible in the numerical study the data are compatible with the expected scaling. However, as emphasized by the insets in Fig. 2, the boundary clearly shows kinks, for instance near $Re = 2250$, or jumps (near $Re = 3800$) on top of the global $1/Re$ scaling.

The much finer scan of the lifetimes in the amplitude-Reynolds number plane near $Re = 3800$ in Fig. 3 shows that these structures are due to folds in the edge of chaos. The two data points to the left and right of the jump in the inset in Fig. 2 are shown as open squares at $Re = 3840$ and $Re = 3875$. The scan at the parameter points indicated reveals regions with long lifetimes, whose boundary can be connected to form the fingers shown by the continuous curve that has been drawn to guide the eye. A kink can then result from an unresolved small fold. This picture is consistent with observations in low-dimensional models where the variations can be studied with much higher resolution [13, 14, 15].

The monitoring of lifetimes can also be used to track the dynamics in the edge of chaos. The studies in [16] suggest that all edge points at a given Reynolds number are connected and lie on the stable manifold of an invariant object that resides in state space between the laminar flow and the turbulent dynamics. To find this invariant object, we repeat the steps from [16]: first, find the amplitude for two initial conditions on either side of the edge of chaos, i.e. one which decays towards the laminar profile and one that swings up to the turbulent flow. These two trajectories shadow one that stays in the edge for all times. After about 200 time units we refine the approximation and determine a new pair of trajectories close to the edge. The pair of initial conditions is found along the ray connecting the approximated state

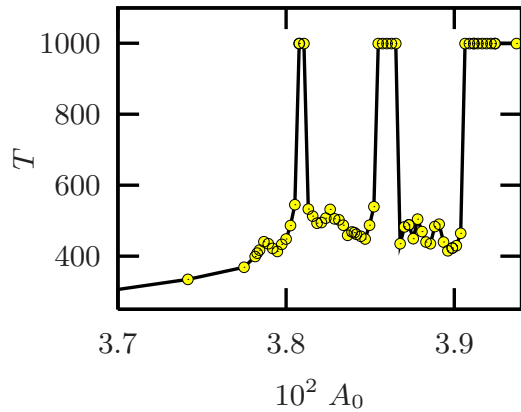


FIG. 1: (Color online) Lifetime T as a function of scaling amplitude $A_0 = \sqrt{E_0}$ at a Reynolds number of $Re = 3875$. The energy E_0 is measured in units of the kinetic energy E_{lam} of the laminar profile generating the same mean downstream velocity. *Edge points* clearly separate regions where the trajectory turns turbulent and the lifetime reaches the numerical cutoff from regions where trajectories directly decay.

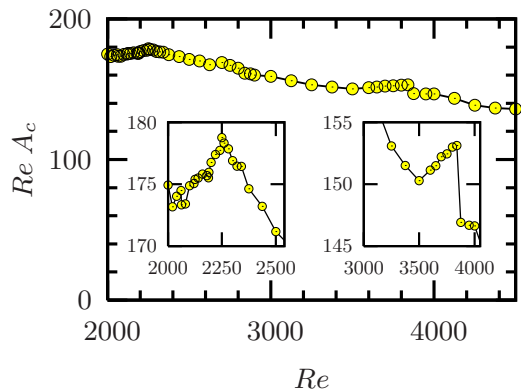


FIG. 2: (Color online) Minimal critical amplitude $A_c = \sqrt{E_c}$ required to trigger turbulence times Re as a function of Re . On top of the proposed $1/Re$ scaling (straight horizontal line) several modulations can be observed. The insets show magnifications of a ‘kink’ at $Re \approx 2200$ (left) and a ‘jump’ at $Re \approx 3800$ (right).

from the previous step (the one escaping to the turbulence) and the laminar profile. Four refinements and the exponential separation in energy within a pair are shown in Fig. 4. The inset shows that we keep their separation below 10^{-8} in energy. As long as the direction in state space defined by the amplitude scaling is not tangent to the edge manifold this technique can be used to obtain arbitrarily long traces of a state that neither decays nor swings up to the turbulence: this trajectory lives in the edge of chaos and should approach the invariant state embedded in the edge of chaos the *edge state*.

The edge state is a relative attractor: it is attracting for initial conditions confined to the edge of chaos, but repelling perpendicular to it. In its simplest form the invariant state is a hyperbolic fixed point and the

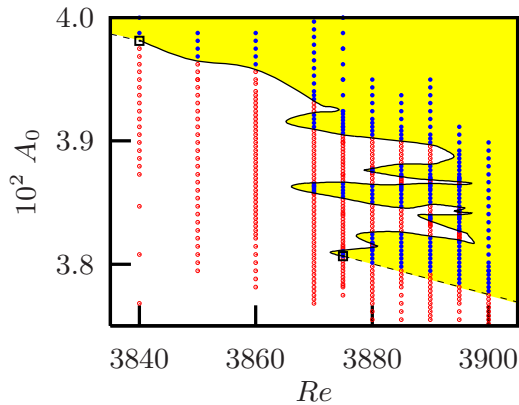


FIG. 3: (Color online) Lifetime landscape in the A_0 - Re plane. Blue filled circles indicate transition to turbulence and red open circles immediate decay. The boundary of the domain of initial conditions that connect to the turbulent ‘state’ (shaded) is indicated by the folded back line. The scaling of the critical amplitude A_c from the inset of Fig. 2 is presented as a black dashed line. The jump in A_c from values near 0.0398 at $Re = 3840$ to 0.0380 at $Re = 3875$ (black open squares) can be directly related to the folds in the stability border.

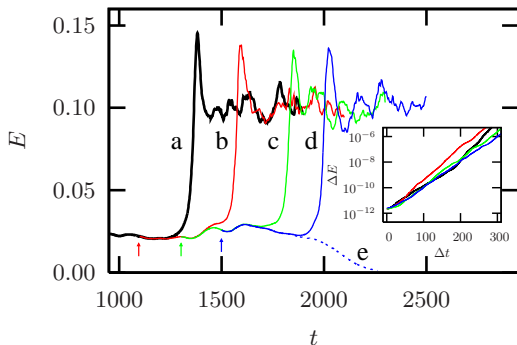


FIG. 4: (Color online) Energy traces of trajectories bounding the edge of chaos. The continuous lines (a-d) show initial conditions that swing up to the turbulent flow and belong to the upper end of the interval. For the last control step, starting at $t = 1500$, also the decaying trajectory (e) from the lower end of the interval is presented as a dotted line. Control steps corresponding to lines (b-d) are indicated by arrows. Trajectory (a) starts at $t = 900$. The inset shows the energy norm of the difference between the two bounding trajectories: the uniform expansion for all segments shows that they all belong to the same invariant state. In absolute values the energy of the difference increase from initially 10^{-12} to at most 10^{-8} during one iteration step.

edge is its stable manifold. Numerical studies of the low-dimensional shear flow models and of chaotic maps show that the edge state can also be a periodic orbit or a chaotic relative attractor.

The continuing modulations in the energy trace in Fig. 4 indicate that the dynamics constrained within the edge of chaos does not relax to a stationary or simply pe-

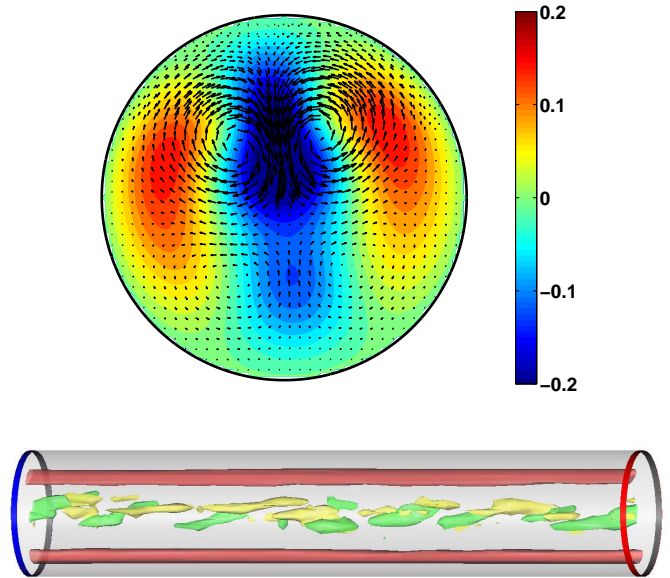


FIG. 5: (Color online) The edge state at $Re = 2875$. Top: Time-averaged cross section perpendicular to the pipe axis. The downstream velocity relative to the parabolic laminar profile is shown in color ranging from red (fast) to blue (slow). In-plane velocity components are indicated by vectors. Bottom: The instantaneous flow field along the axis. Isosurfaces of the downstream velocity (red) indicate the position of the high-speed streaks. Isosurfaces of the downstream vorticity (positive in yellow and negative in green) highlight vortical structures in the center region. The fluid flows from left to right.

riodic state, even when followed up to observation times of more than 2000. Fig. 5 shows a cross section of the flow field, averaged over a time interval of 200 to highlight large scale features. The global structure of the flow field is simple and dominated by two high-speed streaks and a corresponding pair of strong counter-rotating vortices which are located off-center. It shows no discrete rotational symmetry like the travelling waves studied in [9, 10] or the optimal amplification mode in [22].

The side view of an instantaneous snapshot of the edge state in Fig. 5 shows no periodicity in the isosurfaces of the downstream vorticity, again supporting the conclusion that the dynamics in the edge does not settle down to a simple periodic or quasiperiodic travelling wave. The small scale modulations persist and reflect an intrinsically chaotic dynamics of the vortical structures in the center region.

Pipe flow in a domain that is periodically continued in the axial direction has two continuous symmetries of azimuthal and axial translations. Shifted and rotated initial conditions will then give shifted and rotated edge states. Except for these two continuous symmetries, the same edge state is obtained for different initial conditions. It is intriguing that independent of the original velocity field the same relative attractor is reached and that this

relative attractor is dominated by two downstream vortices.

Upon variation of the Reynolds number over the range 2160 . . . 4000 studied here, the overall appearance of the edge state does not change much. We did not detect any bifurcations or transitions between flow topologies, as in the low dimensional model [16]. Energetically, the edge state is clearly separated from both the laminar state (here the energy of the disturbance vanishes exactly) and also from the turbulent state (cf. Fig. 4). However, in view of the transient nature of the turbulent state [24], the stable manifold of the laminar profile and the stable manifold of the edge state have to intermingle tightly in the region with turbulent dynamics.

The form and topology of the edge state suggests that it can be induced experimentally by removing fluid at one point near the wall and by injecting fluid at two points to the left and right of the removal point. This perturbation will then reach into the fluid, forming a pair of vortices not dissimilar to the optimally amplifying ones of Zikanov [22]. The vortices will then draw energy from the base

flow and induce high- and low-speed streaks in the downstream velocity. As in the case of the self-sustained cycle for near wall turbulence [25, 26], one can then anticipate a shear flow instability of the streak arrangement. A direct visualization of this instability is difficult because of the chaotic dynamics of the edge state, but the exponential growth in energy supports the assumption of an instability. Further evolution of the velocity fields then shows that once the energy level of the fully developed turbulence is reached, many more vortices appear, and the velocity field shows more signatures of the symmetric vortex arrangements [11, 27, 28]. It is satisfying to see that the concepts developed in dynamical system theory and verified on low-dimensional models can be transferred so directly to the full, spatially extended systems and that they continue to provide insights into dynamics of this old and puzzling problem.

We thank J. Vollmer and J. Westerweel for helpful discussions, *Hessisches Hochleistungsrechenzentrum* in Darmstadt for computing time, and the Deutsche Forschungsgemeinschaft for support.

-
- [1] O. Reynolds, Phil. Trans. R. Soc. **174**, 935 (1883).
 - [2] T. Mullin and R. R. Kerswell (eds), *Laminar-turbulent transition and finite amplitude solutions* (Springer, Dordrecht, 2004).
 - [3] R. R. Kerswell, Nonlinearity **18**, R17 (2005).
 - [4] B. Eckhardt, T. M. Schneider, B. Hof, and J. Westerweel, Annu. Rev. Fluid Mech. **39**, 447 (2007).
 - [5] L. Boberg and U. Brosa, Z. Naturforsch. **43a**, 697 (1988).
 - [6] A. Darbyshire and T. Mullin, J. Fluid Mech. **289**, 83 (1995).
 - [7] S. Grossmann, Rev. Mod. Phys. **72**, 603 (2000).
 - [8] B. Hof, A. Juel, and T. Mullin, Phys. Rev. Lett. **91**, 244502 (2003).
 - [9] H. Faisst and B. Eckhardt, Phys. Rev. Lett. **91**, 224502 (2003).
 - [10] H. Wedin and R. Kerswell, J. Fluid Mech. **508**, 333 (2004).
 - [11] B. Hof, C. W. H. van Doorne, J. Westerweel, F. T. M. Nieuwstadt, H. Faisst, B. Eckhardt, H. Wedin, R. R. Kerswell, and F. Waleffe, Science **305**, 1594 (2004).
 - [12] L. Trefethen, S. Chapman, D. Henningson, A. Meseguer, T. Mullin, and F. Nieuwstadt, <http://arxiv.org/abs/physics/0007092> (2000).
 - [13] B. Eckhardt and A. Mersmann, Phys. Rev. E **60**, 509 (1999).
 - [14] J. Moehlis, H. Faisst, and B. Eckhardt, New J. Phys. **6**, 56 (2004).
 - [15] J. Moehlis, H. Faisst, and B. Eckhardt, SIAM Appl. Dyn. Syst. **4**, 352 (2005).
 - [16] J. Skufca, J. Yorke, and B. Eckhardt, Phys. Rev. Lett. **96**, 174101 (2006).
 - [17] B. Eckhardt, H. Faisst, A. Schmiegell, and J. Schumacher, in *Advances in Turbulence IX*, edited by I. Castro, P. Hanock, and T. Thomas (Barcelona, 2002), pp. 701–708.
 - [18] T. Itano and S. Toh, J. Phys. Soc. Japan **70**, 703 (2001).
 - [19] S. Toh and T. Itano, J. Fluid Mech. **524**, 249 (2005).
 - [20] A. Schmiegell and B. Eckhardt, Phys. Rev. Lett. **79**, 5250 (1997).
 - [21] H. Faisst and B. Eckhardt, J. Fluid Mech. **504**, 343 (2004).
 - [22] O. Zikanov, Phys. Fluids **8**, 2923 (1996).
 - [23] T. M. Schneider and B. Eckhardt, Chaos **16**, 041103 (2006).
 - [24] B. Hof, J. Westerweel, T. M. Schneider, and B. Eckhardt, Nature **443**, 59 (2006).
 - [25] J. Hamilton, J. Kim, and F. Waleffe, J. Fluid Mech. **287**, 317 (1995).
 - [26] F. Waleffe, Stud. Appl. Math. **95**, 319 (1995).
 - [27] T. M. Schneider, B. Eckhardt, and J. Vollmer, Phys. Rev. E in press (2007).
 - [28] R. R. Kerswell and O. R. Tutty, arXiv:physics/0611009.